Herbert Steinrück
Editor

International Centre for Mechanical Sciences

Asymptotic Methods in Fluid Mechanics: Survey and Recent Advances

CISM Courses and Lectures, vol. 523

SpringerWienNewYork

SpringerWienNewYork

CISM COURSES AND LECTURES

The series presents lecture notes, monographs, edited works and proceedings in the field of Mechanics, Engineering, Computer Science and Applied Mathematics.
Purpose of the series is to make known in the international scientific and technical community results obtained in some of the activities organized by CISM, the International Centre for Mechanical Sciences.

INTERNATIONAL CENTRE FOR MECHANICAL SCIENCES

COURSES AND LECTURES - No. 523

ASYMPTOTIC METHODS IN FLUID MECHANICS: SURVEY AND RECENT ADVANCES

EDITED BY

HERBERT STEINRÜCK
VIENNA UNIVERSITY OF TECHNOLOGY, AUSTRIA

SpringerWienNewYork

This volume contains 119 illustrations

Printed in Italy
SPIN 80022794

All contributions have been typeset by the authors.

ISBN 978-3-7091-0407-1 SpringerWienNewYork

PREFACE

Rational asymptotic methods developed in the fifties and sixties of the last century have played an important role in theoretical physics, mechanics and in particular in fluid mechanics. Among the most powerful methods used in fluid mechanics are the method of matched asymptotic expansions and multiple scales methods. Matched asymptotic expansions are based on the idea of Prandtl's boundary-layer theory. In case of high Reynolds number flows the flow field can be approximated by an inviscid flow with the exception of a thin boundary-layer along the wall where the viscosity has to be taken into account. Both approximations have to match in an intermediate region. In some cases the inviscid flow and the viscous flow in a sub-layer have to be determined simultaneously. Thus one speaks of interacting boundary-layers. An introduction to triple deck problems and recent applications to internal flows, external sub- or supersonic flows, thermal flows and free surface flows will be presented.

Another fruitful application is the theory of separated laminar incompressible flows. Various examples of fluid flows involving separation will be considered, including self-induced separation of the boundary-layer in supersonic gas flows, and incompressible flow separation at the leading edge of an aerofoil. A characteristic feature of a multiple scales problem is that the solution exhibits almost periodic structures whose properties vary on a large scale. Recently, multiple scales methods have been applied to problems in meteorology. Thus well established ad hoc approximations have been verified by applying the method of multiple scales to the basic equations of fluid flow in the atmosphere. It will be demonstrated how a large collection of well-established models of theoretical meteorology can be recovered systematically, how new insight into scale interaction processes is gained, and how the asymptotic analyses provide hints for the construction of accurate and efficient numerical methods. The known limitations of the approach are also discussed.

Many problems in fluid mechanics involve asymptotic expansions in the form of power series. Such expansions necessarily fail to provide terms which are exponentially smaller than all terms in the series. Although small, these missing terms are often of physical importance. How to find such exponentially small terms, using as the

main tool matched asymptotic expansions in the complex plane and Borel summation will be discussed. The techniques will be developed in the context of model problems related to the theory of weakly nonlocal solitary waves which arise in the study of gravity-capillary waves and also for internal waves.

This volume comprises the lecture notes of a course with the title "Asymptotic Methods in Fluid Mechanics - Survey and Recent Advances" held at the Centre for Mechanical Sciences in Udine, September 21-25, 2009. Also included are contributed papers presented at a workshop embedded in the course.

The organizer of the course thanks all lectures and participants of the workshop for their valuable contributions and their cooperation. My personal thanks are to former rector of CISM Prof. Wilhelm Schneider who suggested this course and for his advice during the preparation. Thanks also to the staff of CISM for the perfect organization and the support in producing these lecture notes.

Herbert Steinrück

CONTENTS

Introduction to Matched Asymptotic Expansions

Herbert Steinrück*

* Vienna University of Technology, Institute of Fluid Mechanics and Heat Transfer, Vienna, Austria

Abstract The method of *matched asymptotic expansions* will be presented by applying it to three examples showing the wide applicability of the method.

1 Introduction

The governing equations describing a flow field are in general a set of nonlinear partial differential equations. Only in few situation exact solutions mostly in the form of similarity solutions exist. Thus asymptotic expansions with respect to an appropriate dimensionless parameter (e.g. Reynolds number, Mach number, thickness ratio, ...) which tends to a limiting value (zero or infinity) are sought. Let $\phi(x,\varepsilon)$ with $x \in D \subset R^3$ be a function of a variable x depending on a small, positive parameter ε with $0 < \varepsilon \ll 1$. We call

$$[\phi]^{(n)} = \delta_1(\varepsilon)\phi_1(x) + \delta_2(\varepsilon)\phi_2(x) + \cdots + \delta_n(\varepsilon)\phi_n(x) \tag{1}$$

a n-term asymptotic series of ϕ with respect to $\varepsilon \ll 1$ if the gauge functions $\delta_k(\varepsilon)$ form an asymptotic series, i.e. $\delta_{k+1}(\varepsilon) = o(\delta_k(\varepsilon))$ for $k = 1, \cdots, n-1$ and $\phi(x,\varepsilon) - [\phi^{(n)}] = o(\delta_n(\varepsilon))$.

Note a function $f(\varepsilon)$ is called a small 'o' of the function $g(\varepsilon)$, $f(\varepsilon) = o(g(\varepsilon))$ if $\lim_{\varepsilon\to 0} f(\varepsilon)/g(\varepsilon) = 0$ holds, see Van Dyke (1975). The expansion (1) is called uniformly valid if there exist constants c_1,...,c_n independent of x with

$$\left| \frac{\phi(x,\varepsilon) - [\phi]^{(m)}}{\delta_{m+1}(\varepsilon)} \right| < c_m, \quad m = 1, ..., n. \tag{2}$$

However, the solutions of many perturbation problems in fluid mechanics do not permit an approximation by an asymptotic series of type (1). Such problems are called singularly perturbed. Most of these problems are characterized by two different (length) scales. For example consider the attached high Reynolds number flow. A regular (outer) expansion fails near a

solid surface and a local variable has to be introduced to describe the local behavior near the wall and a local (inner) expansion of the flow field can be found. To get a uniformly valid approximation of the entire flow region both expansions have to match. Thus one speaks of matched asymptotic expansion.

Boundary layers have been first introduced by Prandtl (1904) by explaining the role of viscosity in large Reynolds number flows. As a mathematical tool the method of matched asymptotic expansions has been developed systematically in between the 50s and 70s of the last century, see Kaplun (1967), Lagerström and Van Dyke (1975), Fraenkel (1969)

Matched asymptotic expansions are used if a regular asymptotic expansion fails near located singularities. Then the problem has to be rescaled appropriately by using local variables before expanding its solution asymptotically. Both expansion have to agree in some overlap region, i.e. a region where both expansions hold. We will demonstrate the method by considering three typical examples showing the wide applicability of the method.

Inviscid potential flow around a thin profile. The flow potential is expanded with respect to a small aspect ratio of the profile. At first glance one might think that a regular expansion will be sufficient. However, it turns out that the tentative regular expansion is not uniformly valid near the leading and the trailing edge. Thus local expansions turn out to be necessary to obtain a uniformly valid solution, cf. Van Dyke (1975).

Flow between two rotating discs: Ekman-layer. A common reason for the necessity to introduce a local expansion is that the perturbation parameter multiplies the highest derivative of the unknown function in a differential equation. As a consequence the solution of the limiting differential equation cannot satisfy all required boundary conditions. By introducing a local variable the small coefficient of the highest derivative can be rescaled and the local expansion can satisfy all boundary conditions.

As a representative of that class of problems the flow between two rotating discs in the limit of a small Ekman number will be discussed, see Ungarish (1993).

Model equation: turbulent pipe flow. Here the asymptotic behavior off an ordinary differential equation is analyzed modeling turbulent pipe flow in the limit of large Reynolds numbers. The limiting differential equation is of the same order as the perturbed one. However, the coefficient of the highest derivative vanishes only at the boundary where a boundary

condition has to be satisfied. Thus again a local expansion turns out to be necessary. The matching of the two expansions will be discussed and an short introduction to turbulence asymptotics will be given.

2 Flow around a thin elliptical airfoil $\varepsilon \ll 1$

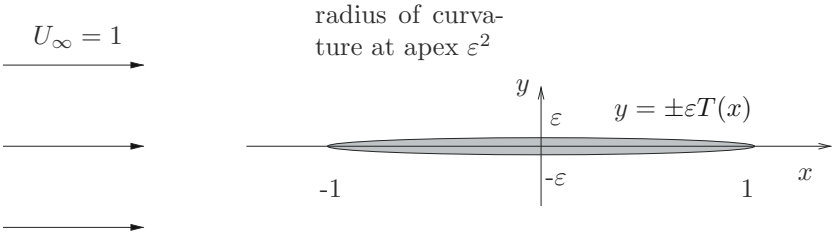

Figure 1. Elliptical thin airfoil

As a first example we consider the two-dimensional inviscid irrotational flow past a thin airfoil. For simplicity we consider a symmetric profile in a uniform free stream parallel to its center line. We place the x-axis of a coordinate system at the centerline of the airfoil such that leading and trailing edge are at $x = \mp 1$ in dimensionless coordinates, respectively. The contour of the profile is given by $y = \pm\varepsilon T(x)$, where ε is the thickness of the airfoil assumed to be small, see figure 1.

The dimensionless flow field can be described by a flow potential $\phi = \phi(x, y)$ where the dimensionless velocity components in x and y direction are given by $u = \phi_x$ and $v = \phi_y$. Thus ϕ is the solution of the potential equation

$$\phi_{xx} + \phi_{yy} = 0 \tag{3}$$

subject to the kinematic boundary condition at the surface of the airfoil

$$\phi_y(x, \pm\varepsilon T(x)) = \pm\varepsilon T'(x)\phi_x(x, \pm\varepsilon T(x)), \quad -1 < x < 1 \tag{4}$$

and the incident flow condition

$$\phi \to x, \quad \text{for} \quad x^2 + y^2 \to \infty. \tag{5}$$

2.1 Asymptotic expansion of the flow potential (regular expansion)

In order to find an asymptotic expansion of the flow potential with respect to a small thickness parameter $\varepsilon \ll 1$ a regular expansion in terms of

powers of ε is employed. In the limiting case $\varepsilon = 0$ the undisturbed parallel flow ($\phi = x$) is obtained. Thus we try to determine a regular expansion in powers of the perturbation parameter ε

$$\phi = x + \varepsilon\phi_1 + \varepsilon^2\phi_2 + \dots, \tag{6}$$

where ϕ_i are the solutions of the potential equation. In order to satisfy the kinematic boundary condition derivatives of the flow potential have to be evaluated at $y = \pm\varepsilon T(x)$. However, the evaluation at $y = \varepsilon T(x)$ is approximated by a Taylor expansion of the corresponding quantity around $(x, 0+)$, i.e.

$$\begin{aligned}\phi_x(x, \varepsilon T(x)) \sim 1 + \varepsilon\phi_{1,x}(x, 0+) + \\ + \varepsilon^2 \left(\phi_{1,xy}(x, 0+)T(x) + \phi_{2,x}(x, 0+)\right) + ...\end{aligned} \tag{7}$$

Thus the expansion of the kinematic boundary conditions yields conditions for the perturbation potentials ϕ_k

$$\phi_{k,y}(x, \pm 0) = \begin{cases} \pm T'(x), & k = 1, \\ \pm(T(x)\phi_{1,x}(x, 0\pm))_x, & k = 2, \\ \pm(T(\phi_{2,x} + \frac{1}{2}TT''))_x, & k = 3, \end{cases} \qquad -1 < x < 1 \tag{8}$$

The incident flow condition requires that flow field vanishes for large $x^2 + y^2 \to \infty$.

$$\phi_i(x, y) \to 0, \quad x, y \to \infty. \tag{9}$$

Note the flow potential of a source at the origin of strength q is $\phi^{(q)} = \frac{q}{2\pi} \ln\sqrt{x^2 + y^2}$. The perturbation potentials ϕ_k can be obtained by placing distributed sources along the centerline of the airfoil on the interval $(-1, 1)$ and one can verify that the corresponding velocity fields can be represented by:

$$u_k(x, y) = \phi_{k,x}(x, y) = \frac{1}{\pi}\int_{-1}^{1} \frac{x - \xi}{(x - \xi)^2 + y^2}\, \phi_{k,y}(\xi, 0)\ \mathrm{d}\xi, \tag{10a}$$

$$v_k(x, y) = \phi_{k,y}(x, y) = \frac{1}{\pi}\int_{-1}^{1} \frac{y}{(x - \xi)^2 + y^2}\, \phi_{k,y}(\xi, 0)\ \mathrm{d}\xi, \tag{10b}$$

cf. Van Dyke (1975). Using the perturbation potentials ϕ_i the surface velocity u_s has the expansion

$$\begin{aligned}u_s(x) = \sqrt{\phi_x^2(x, \pm\varepsilon T(x)) + \phi_y^2(x, \pm\varepsilon T(x))} \sim \\ +\varepsilon\phi_1(x, 0) + \varepsilon^2\left[\phi_{2x}(x, 0) + T(x)T''(x) + \frac{1}{2}T'^2(x)\right] + \cdots \quad .\end{aligned} \tag{11}$$

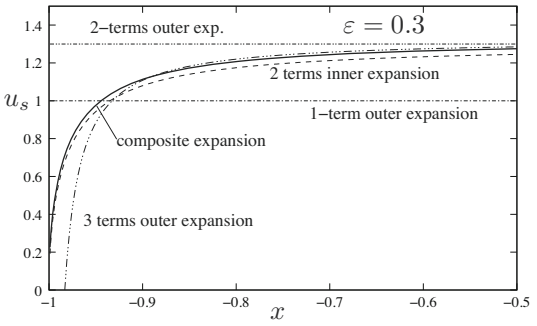

Figure 2. Asymptotic expansion of surface velocity

To be more specific we consider an elliptical airfoil with the shape function $T(x) = \sqrt{1-x^2}$. Using the notation of complex variables $z = x + iy$ the perturbation potentials ϕ_1, ϕ_2 are

$$\phi_1 = \phi_2 = \Re\left(z - \sqrt{z^2-1}\right), \tag{12}$$

where $\Re z$ denotes the real part of a complex number z. In order to make the square root unique the complex plane is sliced along the interval (-1,1). We have $\phi_{1,x}(x, \pm 0) = \phi_{2,x}(x, \pm 0) = \pm 1$. Thus the expansion of the surface velocity

$$u_s(x) \sim 1 + \varepsilon - \frac{\varepsilon^2}{2}\frac{x^2}{1-x^2} + \cdots \tag{13}$$

turns out to be not uniformly valid. If x is close to the leading or trailing edge, say $|x+1| \ll \varepsilon^2$ the second order correction term will become larger than the first, (see figure 2).

It is interesting to note that the flow potential of a source or sink flow at the leading or trailing edge can be added to the perturbation potential ϕ_1. In particular the flow potential

$$\phi_1 = \Re\left(z - \sqrt{z^2-1} - \frac{C}{2\pi}\ln\frac{z+1}{z-1}\right) \tag{14}$$

satisfies all required conditions for an arbitrary constant C.

2.2 Local expansion at leading/trailing edge

Since the expansion presented previously fails near the leading edge we introduce local coordinates to describe the flow field there. A natural length

scale near the leading edge is the radius of curvature of the profile, which in case of the elliptical airfoil is ε^2. Thus we define the local coordinates

$$X = \frac{1+x}{\varepsilon^2}, \quad Y = \frac{y}{\varepsilon^2}, \tag{15}$$

and the local flow potential by $\Phi(X,Y)$ by

$$\phi(x,y) = \phi(-1,0) + \varepsilon^2 \Phi(X,Y). \tag{16}$$

The local potential satisfies again the Laplace equation. The contour of the airfoil written in local coordinates is given by

$$Y = \pm\sqrt{2X + \varepsilon^2 X^2} \sim \sqrt{2X}\left(1 + \frac{\varepsilon^2}{4}X + ...\right). \tag{17}$$

Thus the kinematic boundary condition in local coordinates reads

$$\Phi_Y\left(X, \sqrt{2X - \varepsilon^2 X^2}\right) - \frac{1-\varepsilon^2 X}{\sqrt{2X - \varepsilon^2 X^2}}\Phi_X\left(X, \sqrt{2X - \varepsilon^2 X^2}\right) = 0. \tag{18}$$

We expand the local solution with respect to ε asymptotically

$$\Phi(X,Y) = \Phi_0 + \varepsilon\Phi_1 + \varepsilon^2\Phi_2 + ... \tag{19}$$

and obtain for the first two terms the kinematic boundary condition

$$\Phi_{i,Y}\left(X, \sqrt{2X}\right) - \frac{1}{\sqrt{2X}}\Phi_{i,X}\left(X, \sqrt{2X}\right) = 0, \quad i = 0, 1. \tag{20}$$

This can be interpreted as the kinematic boundary condition for the inviscid flow around a parabola. Due to symmetry the stagnation point is in the apex of the parabola. The flow potential can be determined by conformal mapping, cf. Betz (1964). It is given by

$$\Phi_i = U_{loc,i}\Re\left(Z - 1 + \sqrt{1 - 2Z}\right), \quad i = 0, 1, \tag{21}$$

where the velocities of the free stream $U_{loc,i}$ with $i = 1, 2$ are unknown. They have to be determined by matching with the outer (global) expansion. The expansion of the local surface velocity is given by

$$U_s \sim (U_{loc,0} + \varepsilon U_{loc,1})\sqrt{\frac{2X}{1+2X}}. \tag{22}$$

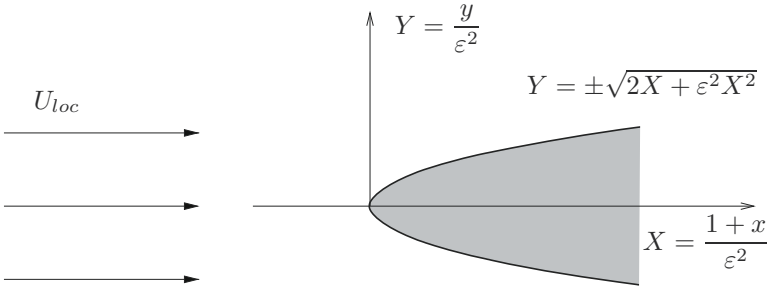

Figure 3. Airfoil in local coordinates

2.3 Matching procedure

We have now determined asymptotic expansions on two different length scales: the outer (global) length scale and a local expansion around the leading edge of the profile, where the radius of curvature is the reference length scale. Both expansions are not uniformly valid in the entire flow domain. The basic hypothesis is that there exists (asymptotically) an overlap where both expansions are valid. Thus we take the outer (global) expansion and rewrite it in the inner (local) variable. For the matching procedure we use the velocity field instead of the flow potential.

We introduce an intermediate variable $\xi(\varepsilon)$ such that

$$z(\varepsilon) = -1 + \varepsilon^2\xi(\varepsilon) \to -1, \quad Z(\varepsilon) = \xi(\varepsilon) \to \infty \quad \text{as} \quad \varepsilon \to 0, \tag{23}$$

and insert it into the global and local expansion, respectively.

The outer expansion of the velocity field in the overlap region is:

$$\phi' \sim 1 - \varepsilon\frac{z}{\sqrt{z^2-1}} + \frac{C}{2\pi}\left(\frac{1}{1+z} - \frac{1}{z-1}\right)\cdots \sim \tag{24}$$

$$1 + \varepsilon\left(1 - \frac{-1+\varepsilon^2\xi}{\sqrt{-2\varepsilon^2\xi + \varepsilon^4\xi^4}} + \frac{C}{\varepsilon^2\xi}\right) \sim 1 + \varepsilon + \frac{1}{\sqrt{-2\xi}} + \frac{C}{\varepsilon\xi}. \tag{25}$$

The local expansion of the velocity field in the overlap region is given by

$$\begin{aligned}\Phi' &\sim (U_{loc,0} + \varepsilon U_{loc,1})\left(1 + \frac{1}{\sqrt{1-2Z}}\right) \\ &\sim U_{loc,0}\left(1 + \frac{1}{\sqrt{-2\xi}}\right) + \varepsilon U_{loc,1}.\end{aligned} \tag{26}$$

Thus both expansions agree in the overlap region if

$$U_{loc,0} = U_{loc,1} = 0, \quad \text{and} \quad C = 0 \tag{27}$$

holds.

Van Dyke (1975) has formalized the matching procedure in the matching principle. Fraenkel (1969) discussed criteria on the inner and outer expansion for the validity of the matching principle. For example when the gauge functions in the outer and inner expansion are powers of the expansion parameter, which is defined as the ratio of the scales of the inner and outer variable, the matching principle holds. Problems may arise when the gauge functions are a combination of powers and logarithmic terms of the perturbation parameter.

Matching principle: n-terms of the outer expansion rewritten in the inner variable and expanded into m terms must agree with m terms of the inner expansion rewritten in the outer variable and expanded into n terms.

$$\Big[\Big[\phi\Big]_{out}^{(n)}\Big]_{in}^{(m)} = \Big[\Big[\phi\Big]_{in}^{(m)}\Big]_{out}^{(n)}. \tag{28}$$

We demonstrate the Matching Principle at the surface velocity of a thin airfoil. We start with the 3 term outer expansion and rewrite it in the local (inner) variables

$$[u_s]_{out}^{(3)} = 1 + \varepsilon - \frac{\varepsilon^2}{2}\frac{x^2}{1-x^2} = 1 + \varepsilon - \frac{1}{X}\frac{(-1+\varepsilon^2 X)^2}{2-\varepsilon^2 X}. \tag{29}$$

Expanding the above expression into two terms yields

$$\Big[\Big[u_s\Big]_{out}^{(2)}\Big]_{in}^{(3)} = 1 - \frac{1}{4X} + \varepsilon. \tag{30}$$

On the other hand two terms of the inner expansion rewritten in the outer variables gives

$$\Big[\Big[u_s\Big]_{in}^{(2)}\Big]_{out}^{(2)} = \left[(1+\varepsilon)\sqrt{\frac{2X}{1+2X}}\right]_{out}^{(2)} = 1 + \varepsilon - \frac{\varepsilon^2}{4(1+x)}. \tag{31}$$

Thus both expressions agree.

2.4 Composite approximation

In order to get a uniformly valid approximation one has to combine the inner and outer expansion. This can be done by adding both expansions. Doing so the overlap region is represented twice. Thus the common part of both expansion has to be subtracted.

$$u_s \sim [u_s]^{(2)}_{in} + [u_s]^{(3)}_{out} - \left[\left[\phi\right]^{(3)}_{out}\right]^{(3)}_{in} = \tag{32}$$

$$= (1+\varepsilon)\sqrt{\frac{2X}{1+2X}} - \frac{\epsilon^2}{2}\frac{x^2}{1-x^2} + \frac{1}{4X}.$$

In figure 2 the outer, the inner expansion and the composite approximation of the surface velocity are shown for $\varepsilon = 0.3$.

3 Flow between rotating discs - Ekman layers

In many applications local expansions have to be introduced since the solution of the limiting problem cannot satisfy all boundary conditions. Often this is due the fact that the small perturbation parameters multiplies the highest derivative of the unknown function in the governing differential equation. As a representative example we study here the incompressible flow between two infinite parallel discs, which rotate coaxially but at different speeds in the limit of a small Ekman number.

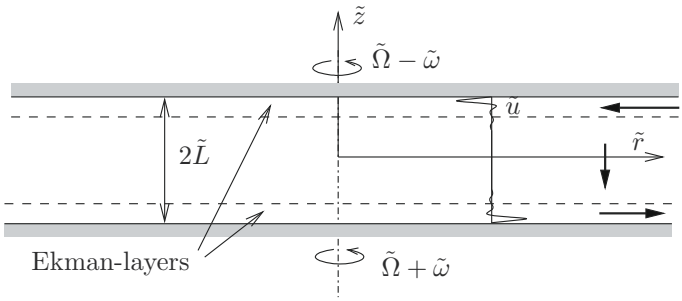

Figure 4. Flow between two coaxially rotating discs

The distance between the two discs is $2\tilde{L}$. Here and in the following we denote dimensional quantities with a tilde. The upper disc rotates with speed $\tilde{\Omega} - \tilde{\omega}$ and the lower with $\tilde{\Omega} + \tilde{\omega}$. We choose a cylindrical coordinate system with the axis of rotation as the z-axis and its origin in the mid-

dle between the two plates. The fluid between the discs is assumed to be incompressible and its kinematic viscosity $\tilde{\nu}$ to be constant.

Thus two independent dimensionless group can be formed: The Ekman number $Ek = \tilde{\nu}/\tilde{\Omega}\tilde{L}^2$ and the Rossby number $Ro = \tilde{\omega}/\tilde{\Omega}$. If the Rossby number is zero both discs rotate at the same angular speed. In that case the fluid between the two discs would do the same. Thus the Rossby number is a measure of the deviation of the solid body rotation of the fluid. Here we will assume that the Rossby number is small.

The Ekman number can be interpreted as the reciprocal value of a Reynolds number based on the reference velocity $\tilde{\Omega}\tilde{L}$. Here we are interested in the limit of small Ekman numbers.

The governing Navier-Stokes equation written in cylindrical coordinates can be found in Schlichting (2000). We use the dimensionless vertical coordinate $Z = \frac{\tilde{z}}{\tilde{L}}$ and introduce the similarity ansatz

$$\tilde{u} = \tilde{r}\tilde{\omega}U(Z), \qquad \tilde{v} = \tilde{r}\tilde{\Omega} + \tilde{r}\tilde{\omega}V(Z), \qquad \tilde{w} = \tilde{L}\tilde{\omega}W(Z), \tag{33a}$$

$$\tilde{p} = \frac{1}{2}\tilde{\rho}\tilde{\Omega}^2\tilde{r}^2 + \frac{1}{2}\tilde{\rho}\tilde{\Omega}\tilde{\omega}\tilde{r}^2 A + \tilde{\rho}\tilde{\Omega}\tilde{\omega}\tilde{L}^2 B(Z). \tag{33b}$$

Thus the Navier-Stokes equation reduce to a set of nonlinear ordinary differential equations for the secondary flow induced by the difference of the angular velocities.

$$Ro\,(U^2 - V^2 + WU_Z) = 2V - A + Ek\,U_{ZZ}, \tag{34a}$$

$$Ro\,(2UV + WV_Z) = -\,2U + Ek\,V_{ZZ}, \tag{34b}$$

$$Ro\,WW_Z = -B_Z + Ek\;W_{ZZ}, \tag{34c}$$

$$2U + W_Z = 0. \tag{34d}$$

At the two discs the no slip boundary conditions have to be satisfied.

$$U(\pm 1) = 0, \quad V(\pm 1) = \mp 1, \quad W(\pm 1) = 0. \tag{35}$$

These are a set of ordinary differential equations for the velocity profiles U, V, W, the pressure profile B and the constant A. At first glance one might think that the six no-slip boundary conditions are not enough. But we have to consider equation (34a), (34b) as second order equations for U and V, respectively. The continuity equation (34d) can be considered as first order equation for the vertical velocity profile W and equation (34c) can be considered as an algebraic equation for the vertical pressure gradient B_Z. Thus in total six boundary conditions are needed to determine U, V, W, B_Z and A .

Assuming a small difference in the speeds of rotation of the two discs (small Rossby number Ro) we can neglect the nonlinear terms and obtain a linear set of ordinary differential equations with constant coefficients.

$$Ek\,U_{ZZ} = A - 2V, \quad Ek\,V_{ZZ} = 2U, \quad W_Z - 2U, \quad B_Z = Ek\,W_{ZZ}. \quad (36)$$

We remark that for positive Ro-numbers the solution can be expanded into a regular power series with respect to powers of Ro.

3.1 Small Ekman numbers

Of course the set of ordinary differential equations (36) can be solved analytically. Here we want to demonstrate how to find an asymptotic solution in the limit $Ek \to 0$.

3.2 Core region

We expand the constant $A = A_0 + Ek^\alpha A_1 + ...$ and the solution (U, V, W) in the core region into powers of the Ekman number Ek

$$\begin{pmatrix} U(Z;Ek) \\ V(Z;Ek) \\ W(Z;Ek) \end{pmatrix} = \begin{pmatrix} \bar{U}_0(Z) \\ \bar{V}_0(Z) \\ \bar{W}_0(Z) \end{pmatrix} + Ek^\alpha \begin{pmatrix} \bar{U}_1(Z) \\ \bar{V}_1(Z) \\ \bar{W}_1(Z) \end{pmatrix} + ... \quad (37)$$

and insert it into (36). Comparing like powers we obtain

$$\bar{U}_i = 0, \quad \bar{V}_i = \frac{A_i}{2}, \quad \bar{W}_i = W_i, \quad i = 0, 1. \quad (38)$$

However, the constants A_0, A_1, W_0 and W_1 remain undetermined yet. Unfortunately (38) cannot satisfy all boundary conditions for V and W.

3.3 Boundary layers

Thus we expect that the solution will vary rapidly near the boundary in order to satisfy the boundary conditions. In order to capture this rapid variation we introduce local variables near the boundaries at $Z = \pm 1$.

$$\eta = \frac{1 - Z}{Ek^\beta}, \quad \zeta = \frac{1 + Z}{Ek^\beta} \quad (39)$$

The independent variable will be stretched with the factor Ek^β. The exponent β will be determined appropriately later.

Setting $U(Z) = \hat{U}(\eta)$ and similarly V and W and inserting into (36) we obtain the differential equations describing the local behavior of the flow near the lower disc.

$$Ek^{1-2\beta}\hat{U}'' = A_0 - 2\hat{V}, \quad Ek^{1-2\beta}\hat{V}'' = 2\hat{U}, \quad Ek^{-\beta}\hat{W}' = \mp 2\hat{U}. \quad (40)$$

We remark that for the local behavior near the upper disc we obtain a similar differential equation. Only the sign in front of $\hat{W}'$ has to be changed. Inspecting the local differential equation and setting $Ek = 0$ we see immediately that a nontrivial differential equation is obtained if $\beta = 1/2$. Thus we expand

$$\begin{pmatrix} U \\ V \\ W \end{pmatrix} \sim \begin{pmatrix} \hat{U}_0(\zeta) \\ \hat{V}_0(\zeta) \\ \hat{W}_0(\zeta) \end{pmatrix} + \sqrt{Ek} \begin{pmatrix} \hat{U}_1(\zeta) \\ \hat{V}_1(\zeta) \\ \hat{W}_1(\zeta) \end{pmatrix} + \cdots \quad . \tag{41}$$

From the boundary condition at the lower disc ($Z = -1$) we obtain the boundary condition for the local expansion

$$\hat{U}_0(0) = \hat{U}_1(0), \quad \hat{V}_0(0) = 1, \quad \hat{V}_1(0) = 0, \quad \hat{W}_0(0) = \hat{W}_1(0). \tag{42}$$

Inserting the expansion (41) into (40) and after some elementary manipulations we obtain a fourth-order differential equation for $\dot{V}_0$

$$\hat{V}_0^{(iv)} + 4\hat{V}_0 = 2A_0, \quad \hat{V}_0(0) = 1, \quad \hat{V}_0''(0) = 0, \tag{43}$$

with the solution

$$\hat{V}_0(\xi) = \frac{A_0}{2} + \left(1 - \frac{A_0}{2}\right) e^{-\xi} \cos\xi + c_1 \sinh\xi \cos\xi + c_2 \cosh\xi \sin\xi. \tag{44}$$

For the radial velocity component we obtain from $\hat{U}_0 = -\frac{1}{2}\hat{V}_0''$

$$\hat{U}_0(\xi) = \left(1 - \frac{A_0}{2}\right) e^{-\xi} \sin\xi - 2c_1 \cosh\xi \sin\xi + 2c_2 \sinh\xi \cos\xi \tag{45}$$

and for the vertical component $\hat{W}_0 = 0$ and

$$\hat{W}_1(\xi) = \left(1 - \frac{A_0}{2}\right) [1 - e^{-\xi}(\sin\xi + \cos\xi)] - \tag{46}$$

$$\frac{c_1 - c_2}{2} \sinh\xi \sin\xi - \frac{c_1 + c_2}{2} (\cosh\xi \cos\xi - 1)$$

follows.

3.4 Matching

Applying the matching principle yields that all quantities in the overlap region between the core layer and the boundary layer have to be constant. Thus we conclude that $c_1 = c_2 = 0$. Furthermore we obtain

$$\bar{U}_0 = 0, \quad \bar{W}_0 = -1 + \frac{A_0}{2}. \tag{47}$$

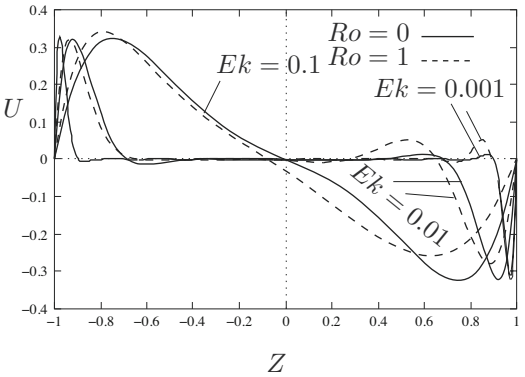

a) radial velocity component

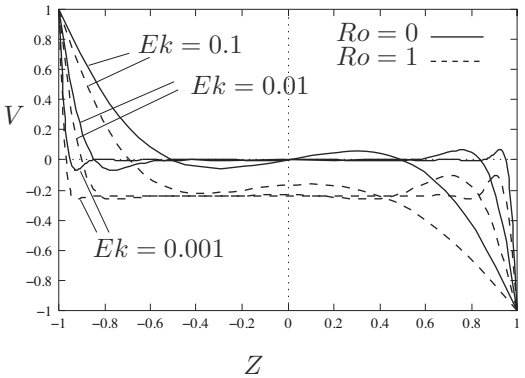

b) azimuthal velocity component

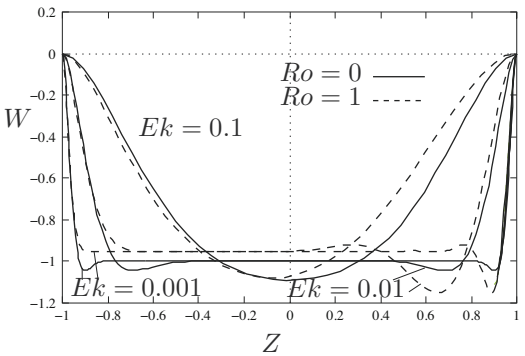

c) vertical velocity component

Figure 5. Velocity profiles between two rotating discs (solution of differential eq. (33)) for $Ek = 0.1$, 0.01, 0.001 and $Ro = 0$, 1.

The analysis of the boundary layer at $Z = 1$ follows the same lines as indicated above. Only the sign in front of the first derivatives and in the boundary condition for the azimuthal velocity V has to be changed.

After matching with the upper layer with the core region we obtain

$$\bar{U}_0 = 0, \quad \bar{W}_0 = -1 - \frac{A_0}{2}. \tag{48}$$

Thus we conclude that $A_0 = 0$ and we have determined all leading order terms of the asymptotic expansion of the velocity profile.

Combining the expansion of the core region with that of the Ekman-layers we obtain the uniformly valid approximation.

$$U \sim e^{-\xi} \sin \xi - e^{-\eta} \sin \eta, \quad V \sim e^{-\xi} \cos \xi - e^{-\eta} \cos \eta, \tag{49a}$$

$$W \sim \sqrt{Ek} \left[-1 + e^{-\xi} (\sin \xi + \cos \xi) + e^{-\eta} (\sin \eta + \cos \eta) \right]. \tag{49b}$$

In figure 5 numerical solutions of the similarity equations (33) are shown for different Ekman- and Rossby numbers. As expected, the velocity profiles exhibit Ekman-layers near the rotating walls.

4 Model equation for fully developed turbulent channel flow

As the third example of matched asymptotic expansions we will study the fully developed turbulent channel flow in the limit of large Reynolds numbers. We expect that the reader is familiar with the basic terminology in turbulent flows, namely the Reynolds decomposition of the flow and pressure field into mean flow, mean pressure and fluctuating velocities and pressure, respectively.

Assuming a fully developed flow, i.e. all averaged flow quantities do not depend on the coordinate $\tilde{x}$ in flow direction the mean velocity $\tilde{u}$ and the shear stress $\tilde{\tau}$ are function of the lateral coordinate $\tilde{y}$ only.

The momentum balance yields an equilibrium between the pressure gradient $\mathrm{d}\tilde{p}/\mathrm{d}\tilde{x}$ and the $\tilde{y}$-derivative of the shear stress $\tilde{\tau}$

$$0 = -\frac{\mathrm{d}\tilde{p}}{\mathrm{d}\tilde{x}} + \frac{\mathrm{d}\tilde{\tau}}{\mathrm{d}\tilde{y}}. \tag{50}$$

The averaged shear stress $\tilde{\tau}$ is the sum of the Reynolds shear stress $\tilde{\tau}_t = -\tilde{\rho}\overline{(\tilde{u}'\tilde{v}')}$ and the viscous stress

$$\tilde{\tau} = \tilde{\tau}_t + \tilde{\mu} \frac{\mathrm{d}\tilde{u}}{\mathrm{d}\tilde{y}}. \tag{51}$$

At the channel wall $\tilde{y} = 0$ the no slip boundary condition $\tilde{u} = 0$ holds and at the centerline $\tilde{y} = \tilde{d}$ due to symmetry the shear stress $\tilde{\tau}$ vanishes. Here we consider the center line velocity $\tilde{u}_c$ as a given quantity and want to determine the velocity profile $\tilde{u} = \tilde{u}(\tilde{y})$ and the pressure gradient, respectively. A more physical boundary condition is that the mean velocity (or volume flux) is prescribed, but for the sake of simplicity of the analysis we prescribe here the center line velocity.

In order to close the problem, a relation between the mean flow $\tilde{u}$ or its derivatives and the turbulent shear stress is missing. There is a vast literature and several approaches how such a closure can be accomplished. We assume here a simple turbulence model for wall bounded shear flows, namely the mixing length model

$$\tilde{\tau}_t = \tilde{\rho}\tilde{l}^2 \left| \frac{\mathrm{d}\tilde{u}}{\mathrm{d}\tilde{y}} \right| \frac{\mathrm{d}\tilde{u}}{\mathrm{d}\tilde{y}}. \tag{52}$$

In case of a channel flow an expression for the mixing length $\tilde{l} = \tilde{l}(\tilde{y}) = \tilde{d}l(y)$ as a function of the dimensionless distance $y = \tilde{y}/\tilde{l}$ from the wall can be found in Schlichting (2000)

$$l(y) = c_0 - \left(2c_0 - \frac{\kappa}{2}\right)(1-y)^2 - \left(\frac{\kappa}{2} - c_0\right)(1-y)^4. \tag{53}$$

Note that the mixing length $\tilde{l}$ vanishes at the wall $\tilde{y} = 0$ and that $l(y) \sim \kappa y + l_2 y^2/2 + O(y^3)$ for $y \ll 1$ holds.

We introduce dimensionless variables by referring the velocity to the center line velocity $\tilde{u}_c$, the shear stress to the double stagnation pressure $\tilde{\rho}\tilde{u}_c^2$, the unknown pressure gradient to $\tilde{\rho}\tilde{u}_c^2/\tilde{d}$.

We define

$$\gamma^2 = -\frac{\tilde{d}}{\tilde{\rho}\tilde{u}_c^2}\frac{\mathrm{d}\tilde{p}}{\mathrm{d}\tilde{x}} = \frac{\tilde{\tau}_w}{\tilde{\rho}\tilde{u}_c^2} = \frac{\tilde{u}_\tau^2}{\tilde{u}_c^2}, \quad \varepsilon = \frac{1}{Re} = \frac{\tilde{\mu}}{\tilde{\rho}\tilde{u}_c\tilde{d}}, \tag{54}$$

where we have made use of the force balance $-\mathrm{d}\tilde{p}/\mathrm{d}\tilde{x} = \tilde{\tau}_w/\tilde{d}$ for a fully developed flow and the definition of the wall shear stress velocity $\tilde{u}_\tau = \sqrt{\tilde{\tau}_w/\tilde{\rho}}$ with $\tilde{\tau}_w$ denoting the wall shear stress. The dimensionless equations reduce to the stress balance

$$0 = \gamma^2 + \frac{\mathrm{d}\tau}{\mathrm{d}y}, \tag{55}$$

and stress relation

$$\tau = \varepsilon\frac{\mathrm{d}u}{\mathrm{d}y} + l(y)^2\left(\frac{\mathrm{d}u}{\mathrm{d}y}\right)^2, \tag{56}$$

subject to the boundary conditions

$$u(0) = 0, \quad u(1) = 1, \quad \tau(1) = 0. \tag{57}$$

Integration of the momentum balance yields

$$\tau(y) = \gamma^2(1 - y). \tag{58}$$

and it remains to solve the first order ordinary differential equation (56) for the velocity profile u and the dimensionless wall shear stress (or negative pressure gradient) γ^2.

4.1 Defect Layer

We expand the solution with respect to small values of ε (large Reynolds numbers). However, we also have to determine γ whose order of magnitude as a function of ε is not obvious. We anticipate that $\gamma = o(1)$ as $\varepsilon \to 0$. From the stress relation we deduce that $\mathrm{d}u/\mathrm{d}y = O(\gamma)$. Thus we expand u

$$u(y, \varepsilon) \sim u_0^{(D)}(y) + \gamma(\varepsilon) u_1^{(D)}(y) + \varepsilon u_2^{(D)}(y). \tag{59}$$

Inserting into the stress relation we obtain that $u_0^{(D)}$ is a constant. However, we have two contradicting boundary conditions to determine $u_0^{(D)}$. For the next order term $u_1^{(D)}$ we obtain from the stress relation

$$1 - y = l(y)^2 \left(\frac{\mathrm{d}u_1^{(D)}}{\mathrm{d}y} \right)^2. \tag{60}$$

Integration yields

$$u_1^{(D)}(y) = \frac{1}{\kappa} \ln y + F^{(D)}(y) + u_1^{(D)}(1), \tag{61}$$

where

$$F^{(D)}(y) = \int_1^y \left(\frac{\sqrt{1 - y'}}{l(y')} - \frac{1}{\kappa y'} \right) \mathrm{d}y' \tag{62}$$

is a smooth bounded function of y on the interval $(0, 1)$.

Now it is obvious to see that $u_1^{(D)}$ is smooth at the centerline $y = 1$ and thus $u_0^{(D)} = 1$ and $u_1^{(D)}(1) = 0$. The velocity profile deviates only by a small velocity defect of order γ from its maximum value at the center line. Therefore this layer is called defect layer. Near the wall $y = 0$ the velocity component $u_1^{(D)}(y)$ is singular. Its asymptotic behavior is given by

$$u_1^{(D)}(y) \sim \frac{1}{\kappa} \ln y + C_D - \frac{\kappa + l_2}{2\kappa^2} y, \quad \text{with} \quad C_D = F^{(D)}(0) \quad \text{as} \quad y \to 0. \tag{63}$$

For the term of order ε we obtain the equation

$$0 = \frac{\mathrm{d}u_1^{(D)}}{\mathrm{d}y} + 2l^2(y)\frac{\mathrm{d}u_1^{(D)}}{\mathrm{d}y}\frac{\mathrm{d}u_2^{(D)}}{\mathrm{d}y}. \tag{64}$$

Integration yields

$$u_2^{(D)} = -\int_1^y \frac{\mathrm{d}y}{2l^2(y)} \sim \frac{1}{2\kappa^2 y} + \frac{l_2}{2\kappa^3}\ln y + C_{D,2} + \cdots \tag{65}$$

with $l_2 = l''(0)$.

4.2 Viscous wall layer

At the wall $y = 0$ the no slip boundary condition cannot be satisfied by the defect expansion (59). Thus we introduce a local variable η

$$u = \gamma u_1^{(v)}(\eta) + \gamma\sigma u_2^{(v)}(\eta) + \cdots, \quad \eta = \frac{y}{\sigma(\varepsilon)} \tag{66}$$

with a stretching $\sigma(\varepsilon)$ which will be determined appropriately. Inserting yields

$$1 = \frac{\mathrm{d}u_1^{(v)}}{\mathrm{d}\eta} + \kappa^2\eta^2\left(\frac{\mathrm{d}u_1^{(v)}}{\mathrm{d}\eta}\right)^2, \quad u_1^{(v)}(0) = 0, \tag{67}$$

$$-\eta - 2l_2\kappa\eta^3\left(\frac{\mathrm{d}u_1^{(v)}}{\mathrm{d}\eta}\right)^2 = \frac{\mathrm{d}u_2^{(v)}}{\mathrm{d}\eta} + 2\kappa^2\eta^2\frac{\mathrm{d}u_1^{(v)}}{\mathrm{d}\eta}\frac{\mathrm{d}u_2^{(v)}}{\mathrm{d}\eta}, \quad u_2^{(v)}(0) = 0, \tag{68}$$

with $\sigma(\varepsilon)\gamma(\varepsilon) = \varepsilon$. Integration of (67) yields

$$u_1^{(v)}(\eta) = \frac{1}{\kappa}\ln\eta + \frac{1}{\kappa}\ln\left(2\kappa + \sqrt{4\kappa^2 + 1/\eta^2}\right). \tag{69}$$

In order to match the viscous layer to the defect layer we consider the asymptotic behavior of $u_1^{(v)}(\eta)$ and $u_2^{(v)}(\eta)$ for $\eta \to \infty$.

$$\frac{\mathrm{d}u_1^{(v)}}{\mathrm{d}\eta} \sim \frac{1}{\kappa\eta} - \frac{1}{2\kappa^2\eta^2} + \frac{1}{8\kappa^3\eta^3} + \cdots, \tag{70a}$$

$$u_1^{(v)}(\eta) = \frac{1}{\kappa}\ln\eta + C_V + \frac{1}{2\kappa^2\eta} - \frac{1}{16\kappa^2\eta^2} + \cdots, \quad \text{with} \quad C_V = \frac{1}{\kappa}(\ln 4\kappa - 1) \tag{70b}$$

$$\frac{\mathrm{d}u_2^{(v)}}{\mathrm{d}\eta} = -\frac{-\eta - \kappa l''\eta^3(\frac{\mathrm{d}u_1^{(v)}}{\mathrm{d}\eta})^2}{1+2\kappa^2\eta^2\frac{\mathrm{d}u_1^{(v)}}{\mathrm{d}\eta}} \sim -\frac{1}{2\kappa} - \frac{l_2}{2\kappa^2} + \frac{l_2}{2\kappa^3\eta} - \frac{3l_2}{8\kappa^4\eta^2} \tag{70c}$$

$$u_2^{(v)}(\eta) \sim -\left(\frac{1}{2\kappa} + \frac{l_2}{2\kappa^2}\right)\eta + C_{V,2} + \frac{l_2}{2\kappa^3}\ln\eta + \frac{3l_2}{16\kappa^4\eta}, \tag{70d}$$

where $C_{V,2}$ is an appropriate constant.

4.3 Matching

Finally it remains to match the velocity profile of the viscous layer with that of the defect layer. Applying the matching principle we have to care when counting the number of terms in the asymptotic expansions. In Fraenkel (1969) it had been shown that the Van Dykes matching principle is still valid when the asymptotic expansion contain besides powers of the perturbation parameter products of powers of ε and and powers of $\ln\varepsilon$. Than all logarithmic term multiplied by the same power of ε have to be considered as one term.

In the present example it will turn out that $\gamma(\varepsilon) \sim O(1/\ln(1/\varepsilon))$. Thus the two term expansion of the defect layer is $1+\gamma U_1^{(D)} + \varepsilon u_2^{(D)}$. Expanding it in the viscous layer variable into two terms and using $\gamma\sigma = \varepsilon$ we obtain

$$\begin{aligned}\left[[u]_D^{(2)}\right]_V^{(2)} &= \left[1+\gamma u_1^{(D)} + \varepsilon u_2^{(D)}\right]_V^{(2)} = \\ &= 1 + \gamma\left(\frac{1}{\kappa}\ln\sigma + \frac{1}{\kappa}\ln\eta + C_D + \frac{1}{2\kappa^2}\frac{1}{\eta}\right) + \\ &+\varepsilon\left(C_{D,2} - \frac{\kappa+l_2}{2\kappa^2}\eta + \frac{l_2}{2\kappa^3}\ln\eta + \frac{l_2}{2\kappa^3}\ln\sigma\right).\end{aligned} \tag{71}$$

Taking two terms of the inner (viscous)-layer expansion $\gamma u_1^{(v)} + \gamma\sigma u_2^{(v)}$, rewriting it in the outer variables and expanding it into two term yields

$$\begin{aligned}\left[[u]_V^{(2)}\right]_D^{(2)} &= \left[\gamma u_1^{(v)} + \gamma\sigma u_2^{(v)}\right]_D^{(2)} = \\ &= \gamma\left(\frac{1}{\kappa}\ln y + C_V - \frac{1}{\kappa}\ln\sigma - \frac{\kappa+l_2}{2\kappa^2}y\right) + \\ &+\gamma\sigma\left(C_{V,2} + \frac{l_2}{2\kappa^3}\ln y - \frac{\sigma}{2\kappa^3}\ln\sigma + \frac{1}{2\kappa^2 y}\right).\end{aligned} \tag{72}$$

Both expressions agree if the matching condition

$$\frac{1}{\gamma} = -\frac{1}{\kappa}\ln\sigma + C_V - C_D - \sigma\left(\frac{l_2}{2\kappa^3}\ln\sigma + C_{D,2} - C_{V,2}\right) \tag{73}$$

is satisfied. Taking only the first order terms of both expansions the well known friction law

$$\frac{1}{\gamma} = \frac{1}{\kappa}\ln\frac{\gamma}{\varepsilon} + C_V - C_D \tag{74}$$

is obtained. It can be interpreted as a relation between the dimensionless wall shear stress γ^2 and the Reynolds number ε^{-1}.

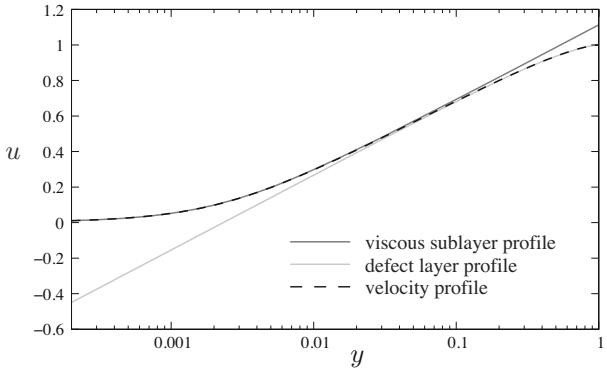

Figure 6. solution of model problem and viscous and defect layer approximation for $\varepsilon = 10^{-4}$

In figure 6 velocity profile as the solution of the force balance with the mixing length model (53) for $\varepsilon = 10^{-4}$, the approximation in the viscous sub-layer and the defect layer is shown in a logarithmic plot. It can be clearly seen that in the overlap region (here from 0.02 to 0.2) viscous and defect expansion agree. In the overlap region both expansions can be represented by a logarithmic velocity profile.

4.4 Turbulence asymptotics

Here we have considered a very simple turbulent shear flow and have made used of a simple turbulence model to reveal the asymptotic structure of flows near the wall. However, the weak point of this approach is the assumption of a turbulence model.

The traditional approach for the limit of large Reynolds numbers is that one considers the shear rate in the overlap region of the viscous and the

defect layer. From dimensional analysis one obtains

$$\frac{\tilde{y}}{\tilde{u}_\tau}\frac{\mathrm{d}\tilde{u}}{\mathrm{d}\tilde{y}} = \Phi(y, y_+), \quad \text{with} \quad y_+ = \frac{\tilde{y}\tilde{u}_\tau}{\tilde{\nu}}, \quad y = \frac{\tilde{y}}{\tilde{d}}. \tag{75}$$

Note that $y_+/y = \tilde{u}_\tau \tilde{d}/\tilde{\nu} = Re_\tau$. To get the behavior of Φ in the overlap region we have to consider the double limit $y_+ \to \infty, y \to 0$. Following von Karman (1930) we assume that this limit exists and its value is the reciprocal value of the von Karman constant,

$$\lim_{y_+\to\infty, y\to 0} \Phi(y, y_+) = \Phi(\infty, 0) = \frac{1}{\kappa}. \tag{76}$$

Integration of (76) yields the logarithmic velocity profile in the overlap region. We emphasize that the existence of the limit (76) from a theoretical point of view is a nontrivial assumption (similarity of the first kind, see Barenblatt (1996). However, the logarithmic law, if interpreted correctly, is in excellent agreement with measured velocity profiles. Thus it can be considered as an empirical fact. On the other hand there are authors , e. g. Barenblatt (1996), who question the logarithmic law. Barenblatt (1996) considers that the limit (76) does not exist, but that the function Φ is a sophisticated power function of the Reynolds number (similarity of the second kind). Instead of the logarithmic velocity profile these authors obtain a power-law with an Reynolds-number dependent exponent. Although according to Barenblatt (1996) the power law seems to reproduce some data even better than the log-law it is a dead end from the asymptotic point of view since it does not comply with the requirements of a rational asymptotic expansion.

In modern papers concerning turbulence asymptotics the order of arguments is reversed, see Walker (1998), Kluwick and Scheichl (2009). Usually the dimensionless wall shear stress velocity $\gamma = u_\tau/U_{ref}$ is considered as a small perturbation parameter and the existence of a viscous sub-layer together with the log-law in the overlap region is postulated.

5 Conclusions

We have given an introduction to the method of matched asymptotic expansion by analyzing three different problems of fluid mechanics. Characteristic to all examples is the appearance of different length scales and that a uniformly valid asymptotic approximation can be constructed employing the matching principle.

Bibliography

G. I. Barenblatt. *Scaling, self-similarity and intermediate asymptotics.* Cambridge Univ. Press, 1996.

A. Betz. *Konforme Abbildungen.* Springer, 2nd edition, 1964.

L. E. Fraenkel. On the method of matched asymptotic expansions, part i: A matching principle. *Proc. Camb. Phil. Soc.*, 65:209–231, 1969.

S. Kaplun. In P.A. Lagerstrom, L. N. Howard, and C. S. Liu, editors, *Fluid Mechanics and Singular Perturbation.* Academic Press, 1967.

A. Kluwick and B. Scheichl. High-Reynolds-Number Asymptotics of Turbulent Boundary Layers: From Fully Attached to Marginally Separated Flows. In A. Hegarty, N. Kopteva, E. O'Riordan, and M. Stynes, editors, *BAIL 2008 - Boundary and Interior Layers*, volume 69 of *Lecture Notes in Computational Science and Engineering*, pages 3–22, 2009.

L. Prandtl. Über Flüssigkeitsbewegung bei sehr kleiner Reibung. In *Verhandl. d. III. Intern. Mathem. Kongresses, Heidelberg*, pages 484–491, 1904.

K. Schlichting, H. Gersten. *Boundary-layer theory.* Springer, 8th edition, 2000.

M. Ungarish. *Hydromechanics of Suspensions.* Springer, 1993.

M. Van Dyke. *Perturbation Methods in Fluid Mechanics.* The Parabolic Press, Stanford, annoted edition edition, 1975.

Th. von Karman. Mechanische Ähnlichkeit und Turbulenz. *Ges. Wiss. Göttingen, Math.-Phys. Kl.*, pages 58–76, 1930.

J. D. A. Walker. Turbulent boundary layers ii: Further developments. In A. Kluwick, editor, *Recent Advances in Boundary Layer Therory*, volume 390 of *CISM Courses and Lectures*, pages 145–230. Springer, 1998.

Asymptotic Methods For PDE Problems In Fluid Mechanics and Related Systems With Strong Localized Perturbations In Two-Dimensional Domains

Michael J. Ward[*‡] and Mary-Catherine Kropinski[†‡]

[*] Department of Mathematics University of British Columbia, Vancouver, B.C., Canada

[†] Department of Mathematics, Simon Fraser University, Burnaby, B.C., Canada

1 Introduction

The method of matched asymptotic expansions is a powerful systematic analytical method for asymptotically calculating solutions to singularly perturbed PDE problems. It has been successfully used in a wide variety of applications (cf. Kevorkian and Cole (1993), Lagerstrom (1988), Dyke (1975)). However, there are certain special classes of problems where this method has some apparent limitations.

In particular, for singular perturbation PDE problems leading to infinite logarithmic series in powers of $\nu = -1/\log\varepsilon$, where ε is a small positive parameter, it is well-known that this method may be of only limited practical use in approximating the exact solution accurately. This difficulty stems from the fact that $\nu \to 0$ very slowly as ε decreases. Therefore, unless many coefficients in the infinite logarithmic series can be obtained analytically, the resulting low order truncation of this series will typically not be very accurate unless ε is very small. Singular perturbation problems involving infinite logarithmic expansions arise in many areas of application in two-dimensional spatial domains including, low Reynolds number fluid flow past bodies of cylindrical cross-section, low Peclet number convection-diffusion problems with localized obstacles, and the calculation of the mean first passage time for Brownian motion in the presence of small traps, etc.

In this article we survey consider various singularly perturbed PDE problems in two-dimensional spatial domains where hybrid asymptotic-numerical methods have been formulated and implemented to effectively 'sum' infinite logarithmic expansions. Some of the problems considered herein directly relate to fluid mechanics, whereas other problems arise in different scientific

contexts. One primary goal of this chapter is to highlight how a common analytical framework can be used to treat a diverse class of problems having strong localized perturbations in two-dimensional domains.

2 Infinite Logarithmic Expansions: Simple Pipe Flow

We first consider the simple model problem of Titcombe and Ward (1999) to illustrate some main ideas for treating PDE problems with infinite logarithmic expansions. We consider steady, incompressible, laminar flow in a straight pipe containing a thin core. Both the pipe and the core have a constant cross-section of arbitrary shape, and thus the problem is two-dimensional. With these assumptions, the pipe flow is unidirectional and the velocity component w in the axial direction satisfies (cf. Ward-Smith (1980))

$$\triangle w = -\beta\,, \quad \mathbf{x} \in \Omega\backslash\Omega_\varepsilon\,, \tag{1a}$$

$$w = 0\,, \quad \mathbf{x} \in \partial\Omega\,, \tag{1b}$$

$$w = 0\,, \quad \mathbf{x} \in \partial\Omega_\varepsilon\,. \tag{1c}$$

Here $\Omega \in \mathbb{R}^2$ is the dimensionless pipe cross-section and Ω_ε is the cross-section of the thin core. We assume that Ω_ε has radius $\mathcal{O}(\varepsilon)$ and that $\Omega_\varepsilon \to \mathbf{x}_0$ uniformly as $\varepsilon \to 0$, where $\mathbf{x}_0 \in \Omega$. We denote the scaled subdomain that results from an $\mathcal{O}(\varepsilon^{-1})$ magnification of the length scale of Ω_ε by $\Omega_1 \equiv \varepsilon^{-1}\Omega_\varepsilon$. In (1a), β is defined in terms of the dynamic viscosity μ of the fluid and the constant pressure gradient dp/dz along the channel by $\beta \equiv -\mu^{-1}dp/dz$. In terms of w, the mean flow velocity $\bar{w}$ is defined by

$$\bar{w} \equiv \frac{1}{A_\Omega}\int_{\Omega\backslash\Omega_\varepsilon} w\, d\mathbf{x}\,. \tag{2}$$

Here A_Ω is the cross-sectional area of the pipe-core geometry. For laminar flow in pipes of non-circular cross-section, with or without cores, the friction coefficient f is expressed in terms of $\bar{w}$ by $f \equiv -L(dp/dz)/(2\rho\bar{w}^2)$ (cf. Ward-Smith (1980)). As a remark, the Reynolds number is defined by $\mathrm{Re} \equiv \bar{w}L\rho/\mu$, where ρ is the density of the fluid. Laminar flow occurs for Reynolds numbers in the approximate range $0 < \mathrm{Re} < 2000$. In the definition of Re, L is a characteristic diameter defined by $L = 4A_\Omega/P_\Omega$, where P_Ω is the wetted perimeter of the pipe and the core.

The asymptotic solution to (1) is constructed in two different regions: an outer region defined at an $\mathcal{O}(1)$ distance from the perturbing core, and an inner region defined in an $\mathcal{O}(\varepsilon)$ neighborhood of the thin core Ω_ε. The

analysis below will show how to calculate the sum of all the logarithmic terms for w in in the limit $\varepsilon \to 0$ of small core radius.

In the outer region we expand the solution to (1) as

$$w(\mathbf{x};\varepsilon) = W_0(\mathbf{x};\nu) + \sigma(\varepsilon)W_1(\mathbf{x};\nu) + \cdots . \tag{3}$$

Here $\nu = \mathcal{O}(1/\log\varepsilon)$ is a gauge function to be chosen, and we assume that $\sigma \ll \nu^k$ for any $k > 0$ as $\varepsilon \to 0$. Thus, W_0 contains all of the logarithmic terms in the expansion. Substituting (3) into (1a) and (1b), and letting $\Omega_\varepsilon \to \mathbf{x}_0$ as $\varepsilon \to 0$, we get that W_0 satisfies

$$\triangle W_0 = -\beta\,, \quad \mathbf{x} \in \Omega\backslash\{\mathbf{x}_0\}\,, \tag{4a}$$

$$W_0 = 0\,, \quad \mathbf{x} \in \partial\Omega\,, \tag{4b}$$

$$W_0 \quad \text{is singular as} \quad \mathbf{x} \to \mathbf{x}_0\,. \tag{4c}$$

The matching of the outer and inner expansions will determine a singularity behavior for W_0 as $\mathbf{x} \to \mathbf{x}_0$.

In the inner region near Ω_ε we introduce the inner variables

$$\mathbf{y} = \varepsilon^{-1}(\mathbf{x} - \mathbf{x}_0)\,, \qquad v(\mathbf{y};\varepsilon) = W(\mathbf{x}_0 + \varepsilon\mathbf{y};\varepsilon)\,. \tag{5}$$

If we naively assume that $v = \mathcal{O}(1)$ in the inner region, we obtain the leading-order problem for v that $\triangle_{\mathbf{y}} v = 0$ outside Ω_1, with $v = 0$ on $\partial\Omega_1$ and $v \to W_0(\mathbf{x}_0)$ as $|\mathbf{y}| \to \infty$, where $\triangle_{\mathbf{y}}$ denotes the Laplacian in the $\mathbf{y}$ variable. This far-field condition as $|\mathbf{y}| \to \infty$ is obtained by matching v to the outer solution. However, in two-dimensions there is no solution to this problem since the Green's function for the Laplacian grows logarithmically at infinity. To overcome this difficulty, we require that $v = \mathcal{O}(\nu)$ in the inner region and we allow v to be logarithmically unbounded as $|\mathbf{y}| \to \infty$. Therefore, we expand v as

$$v(\mathbf{y};\varepsilon) = V_0(\mathbf{y};\nu) + \mu_0(\varepsilon)V_1(\mathbf{y}) + \cdots , \tag{6a}$$

where we write V_0 in the form

$$V_0(\mathbf{y};\nu) = \nu\gamma v_c(\mathbf{y})\,. \tag{6b}$$

Here $\gamma = \gamma(\nu)$ is a constant to be determined with $\gamma = \mathcal{O}(1)$ as $\nu \to 0$, and we assume that $\mu_0 \ll \nu^k$ for any $k > 0$ as $\varepsilon \to 0$. Substituting (5) and (6) into (1a) and (1c), and allowing $v_c(\mathbf{y})$ to grow logarithmically at infinity, we obtain that $v_c(\mathbf{y})$ satisfies

$$\triangle_{\mathbf{y}} v_c = 0\,, \quad \mathbf{y} \notin \Omega_1\,; \qquad v_c = 0\,, \quad \mathbf{y} \in \partial\Omega_1\,, \tag{7a}$$

$$v_c \sim \log|\mathbf{y}|\,, \quad \text{as} \quad |\mathbf{y}| \to \infty\,. \tag{7b}$$

The unique solution to (7) has the following far-field asymptotic behavior:

$$v_c(\mathbf{y}) \sim \log|\mathbf{y}| - \log d + \frac{\mathbf{p}\cdot\mathbf{y}}{|\mathbf{y}|^2} + \cdots, \quad \text{as} \quad |\mathbf{y}| \to \infty\,. \tag{7c}$$

The constant $d > 0$, called the logarithmic capacitance of Ω_1, depends on the shape of Ω_1 but not on its orientation. The vector $\mathbf{p}$ is called the dipole vector. Numerical values for d for different shapes of Ω_1 are given in Ransford (1995), and some of these are reproduced in Table 1. A boundary integral method to compute d for arbitrarily-shaped domains Ω_1 is described and implemented in Dijkstra and Hochstenbach (2008).

Table 1. The logarithmic capacitance, or shape-dependent parameter, d, for some cross-sectional shapes of $\Omega_1 = \varepsilon^{-1}\Omega_\varepsilon$.

Shape of $\Omega_1 \equiv \varepsilon^{-1}\Omega_\varepsilon$	Logarithmic Capacitance d
circle, radius a	$d = a$
ellipse, semi-axes a, b	$d = \frac{a+b}{2}$
equilateral triangle, side h	$d = \frac{\sqrt{3}\,\Gamma\left(\frac{1}{3}\right)^3 h}{8\pi^2} \approx 0.422h$
isosceles right triangle, short side h	$d = \frac{3^{3/4}\Gamma\left(\frac{1}{4}\right)^2 h}{2^{7/2}\pi^{3/2}} \approx 0.476h$
square, side h	$d = \frac{\Gamma\left(\frac{1}{4}\right)^2 h}{4\pi^{3/2}} \approx 0.5902h$

The leading-order matching condition between the inner and outer solutions will determine the constant γ in (6b). Upon writing (7c) in outer variables and substituting into (6b), we get the far-field behavior

$$v(\mathbf{y};\varepsilon) \sim \gamma\nu\left[\log|\mathbf{x}-\mathbf{x}_0| - \log(\varepsilon d)\right] + \cdots, \quad \text{as} \quad |\mathbf{y}| \to \infty\,. \tag{8}$$

Choosing

$$\nu(\varepsilon) = -1/\log(\varepsilon d)\,, \tag{9}$$

and matching (8) to the outer expansion (3) for W, we obtain the singularity condition for W_0,

$$W_0 = \gamma + \gamma\nu\log|\mathbf{x}-\mathbf{x}_0| + o(1)\,, \quad \text{as} \quad \mathbf{x} \to \mathbf{x}_0\,. \tag{10}$$

The singularity behavior in (10) specifies both the regular and singular part of a Coulomb singularity. As such, it provides one constraint for the determination of γ. More specifically, the solution to (4) together with (10) must determine γ, since for a singularity condition of the form $W_0 \sim$

$S \log|\mathbf{x}-\mathbf{x}_0| + R$ for an elliptic equation, the constant R is not arbitrary but is determined as a function of S, $\mathbf{x}_0$, and Ω.

The solution for W_0 is decomposed as

$$W_0(\mathbf{x};\nu) = W_{0H}(\mathbf{x}) - 2\pi\gamma\nu G_d(\mathbf{x};\mathbf{x}_0)\,. \tag{11}$$

Here $W_{0H}(\mathbf{x})$ is the smooth function satisfying the unperturbed problem

$$\triangle W_{0H} = -\beta\,, \quad \mathbf{x}\in\Omega\,; \qquad W_{0H} = 0\,, \quad \mathbf{x}\in\partial\Omega\,. \tag{12}$$

In (11), $G_d(\mathbf{x};\mathbf{x}_0)$ is the Dirichlet Green's function satisfying

$$\triangle G_d = -\delta(\mathbf{x}-\mathbf{x}_0)\,, \quad \mathbf{x}\in\Omega\,; \qquad G_d = 0\,, \quad \mathbf{x}\in\partial\Omega\,, \tag{13a}$$

$$G_d(\mathbf{x};\mathbf{x}_0) = -\frac{1}{2\pi}\log|\mathbf{x}-\mathbf{x}_0| + R_d(\mathbf{x}_0;\mathbf{x}_0) + o(1)\,, \quad \text{as} \quad \mathbf{x}\to\mathbf{x}_0\,. \tag{13b}$$

Here $R_{d00} \equiv R_d(\mathbf{x}_0;\mathbf{x}_0)$ is the regular part of the Dirichlet Green's function $G_d(\mathbf{x};\mathbf{x}_0)$ at $\mathbf{x}=\mathbf{x}_0$. This regular part is also known as either the self-interaction term or the Robin constant (cf. Bandle and Flucher (1996)).

Upon substituting (13b) into (11) and letting $\mathbf{x}\to\mathbf{x}_0$, we compare the resulting expression with (10) to obtain that γ is given by

$$\gamma = \frac{W_{0H}(\mathbf{x}_0)}{1+2\pi\nu R_{d00}}\,. \tag{14}$$

Therefore, for this problem, γ is determined as the sum of a geometric series in ν. The range of validity of (14) is limited to values of ε for which $2\pi\nu|R_{d00}| < 1$. This yields,

$$0 < \varepsilon < \varepsilon_c\,, \qquad \varepsilon_c \equiv \frac{1}{d}\exp\left[2\pi R_{d00}\right]\,. \tag{15}$$

We summarize our result as follows:
Principal Result 1: For $\varepsilon \ll 1$, the outer expansion for (1) is

$$w \sim W_0(\mathbf{x};\nu) = W_{0H}(\mathbf{x}) - \frac{2\pi\nu W_{0H}(\mathbf{x}_0)}{1+2\pi\nu R_{d00}} G_d(\mathbf{x};\mathbf{x}_0)\,, \quad \text{for} \quad |\mathbf{x}-\mathbf{x}_0| = \mathcal{O}(1)\,, \tag{16a}$$

and the inner expansion with $\mathbf{y} = \varepsilon^{-1}(\mathbf{x}-\mathbf{x}_0)$ is

$$w \sim V_0(\mathbf{y};\nu) = \frac{\nu W_{0H}(\mathbf{x}_0)}{1+2\pi\nu R_{d00}} v_c(\mathbf{y})\,, \quad \text{for} \quad |\mathbf{x}-\mathbf{x}_0| = \mathcal{O}(\varepsilon)\,. \tag{16b}$$

Here $\nu = -1/\log(\varepsilon d)$, d is defined in (7c), $v_c(\mathbf{y})$ satisfies (7), and W_{0H} satisfies the unperturbed problem (12). Also $G_d(\mathbf{x};\mathbf{x}_0)$ and $R_{d00} \equiv R_d(\mathbf{x}_0;\mathbf{x}_0)$ are the Dirichlet Green's function and its regular part satisfying (13).

This formulation is referred to as a hybrid asymptotic-numerical method since it uses the asymptotic analysis as a means of reducing the original problem (1) with a hole to the simpler asymptotically related problem (4) with singularity behavior (10). This related problem does not have a boundary layer structure and so is easy to solve numerically. The numerics required for the hybrid problem involve the computation of the unperturbed solution W_{0H} and the Dirichlet Green's function $G_d(\mathbf{x};\mathbf{x}_0)$. In terms of G_d we then identify its regular part $R_d(\mathbf{x}_0;\mathbf{x}_0)$ at the singular point. From the solution to the canonical inner problem (7) we then compute the logarithmic capacitance, d. The result (16a) then shows that the asymptotic solution only depends on the product of εd and not on ε itself. This feature allows for an asymptotic equivalence between holes of different cross-sectional shape, based on an effective 'radius' of the cylinder. This equivalence is known as Kaplun's equivalence principle (cf. Kaplun (1957), Kropinski et al. (1995)).

An advantage of the hybrid method over the traditional method of matched asymptotic expansions is that the hybrid formulation is able to sum the infinite logarithmic series and thereby provide an accurate approximate solution. From another viewpoint, the hybrid problem is much easier to solve numerically than the full singularly perturbed problem (1). For the hybrid method a change of the shape of Ω_1 requires us to only re-calculate the constant d. This simplification does not occur in a full numerical approach.

We now outline how Principal Result 1 can be obtained by a direct summation of a conventional infinite-order logarithmic expansion for the outer solution given in the form

$$W \sim W_{0H}(\mathbf{x}) + \sum_{j=1}^{\infty} \nu^j W_{0j}(\mathbf{x}) + \mu_0(\varepsilon) W_1 + \cdots , \tag{17}$$

with $\mu_0(\varepsilon) \ll \nu^k$ for any $k > 0$. By formulating a similar series for the inner solution, we will derive a recursive set of problems for the W_{0j} for $j \geq 0$ from the asymptotic matching of the inner and outer solutions. We will then sum this series to re-derive the result in Principal Result 1.

In the outer region we expand the solution to (1) as in (17). In (17), $\nu = \mathcal{O}(1/\log\varepsilon)$ is a gauge function to be chosen, while the smooth function W_{0H} satisfies the unperturbed problem (12) in the unperturbed domain. By substituting (17) into (1a) and (1b), and letting $\Omega_\varepsilon \to \mathbf{x}_0$ as $\varepsilon \to 0$, we

get that W_{0j} for $j \geq 1$ satisfies

$$\triangle W_{0j} = 0\,, \quad \mathbf{x} \in \Omega \backslash \{\mathbf{x}_0\}\,, \tag{18a}$$

$$W_{0j} = 0\,, \quad \mathbf{x} \in \partial\Omega\,, \tag{18b}$$

$$W_{0j} \quad \text{is singular as} \quad \mathbf{x} \to \mathbf{x}_0\,. \tag{18c}$$

The matching of the outer and inner expansions will determine a singularity behavior for W_{0j} as $\mathbf{x} \to \mathbf{x}_0$ for each $j \geq 1$.

In the inner region near Ω_ε we introduce the inner variables

$$\mathbf{y} = \varepsilon^{-1}(\mathbf{x} - \mathbf{x}_0)\,, \qquad v(\mathbf{y};\varepsilon) = W(\mathbf{x}_0 + \varepsilon\mathbf{y};\varepsilon)\,. \tag{19}$$

We then pose the explicit infinite-order logarithmic inner expansion

$$v(\mathbf{y};\varepsilon) = \sum_{j=0}^{\infty} \gamma_j \nu^{j+1} v_c(\mathbf{y})\,. \tag{20}$$

Here γ_j are ε-independent coefficients to be determined. Substituting (20) and (1a) and (1c), and allowing $v_c(\mathbf{y})$ to grow logarithmically at infinity, we obtain that $v_c(\mathbf{y})$ satisfies (7) with far-field behavior (7c).

Upon using the far-field behavior (7c) in (20), and writing the resulting expression in terms of the outer variable $\mathbf{x} - \mathbf{x}_0 = \varepsilon\mathbf{y}$, we obtain that

$$v \sim \gamma_0 + \sum_{j=1}^{\infty} \nu^j \left[\gamma_{j-1} \log|\mathbf{x} - \mathbf{x}_0| + \gamma_j\right]\,. \tag{21}$$

The matching condition between the infinite-order outer expansion (17) as $\mathbf{x} \to \mathbf{x}_0$ and the far-field behavior (21) of the inner expansion is that

$$W_{0H}(\mathbf{x}_0) + \sum_{j=1}^{\infty} \nu^j W_{0j}(\mathbf{x}) \sim \gamma_0 + \sum_{j=1}^{\infty} \nu^j \left[\gamma_{j-1} \log|\mathbf{x} - \mathbf{x}_0| + \gamma_j\right]\,. \tag{22}$$

The leading-order match yields that

$$\gamma_0 = W_{0H}(\mathbf{x}_0)\,. \tag{23}$$

The higher-order matching condition, from (22), shows that the solution W_{0j} to (18) must have the singularity behavior

$$W_{0j} \sim \gamma_{j-1} \log|\mathbf{x} - \mathbf{x}_0| + \gamma_j\,, \quad \text{as} \quad \mathbf{x} \to \mathbf{x}_0\,. \tag{24}$$

The unknown coefficients γ_j for $j \geq 1$, starting with $\gamma_0 = W_{0H}(\mathbf{x}_0)$, are determined recursively from the infinite sequence of problems (18) and (24)

for $j \geq 1$. The explicit solution to (18) with $W_{0j} \sim \gamma_{j-1} \log|\mathbf{x}-\mathbf{x}_0|$ as $\mathbf{x} \to \mathbf{x}_0$ is given explicitly in terms of $G_d(\mathbf{x};\mathbf{x}_0)$ of (13) as

$$W_{0j}(\mathbf{x}) = -2\pi\gamma_{j-1} G_d(\mathbf{x};\mathbf{x}_0)\,. \tag{25}$$

Next, we expand (25) as $\mathbf{x} \to \mathbf{x}_0$ and compare it with the required singularity structure (24). This yields

$$-2\pi\gamma_{j-1}\left[-\frac{1}{2\pi}\log|\mathbf{x}-\mathbf{x}_0| + R_{d00}\right] \sim \gamma_{j-1}\log|\mathbf{x}-\mathbf{x}_0| + \gamma_j\,, \tag{26}$$

where $R_{d00} \equiv R_d(\mathbf{x}_0;\mathbf{x}_0)$. By comparing the non-singular parts of (26), we obtain a recursion relation for the γ_j, valid for $j \geq 1$, given by

$$\gamma_j = (-2\pi R_{d00})\,\gamma_{j-1}\,, \qquad \gamma_0 = W_{0H}(\mathbf{x}_0)\,, \tag{27}$$

which has the explicit solution

$$\gamma_j = [-2\pi R_{d00}]^j\, W_{0H}(\mathbf{x}_0)\,, \quad j \geq 0\,. \tag{28}$$

Finally, to obtain the outer solution we substitute (25) and (28) into (17) to obtain

$$\begin{aligned} w - W_{0H}(\mathbf{x}) &\sim \sum_{j=1}^{\infty} \nu^j\,(-2\pi\gamma_{j-1})\,G_d(\mathbf{x};\mathbf{x}_0) = -2\pi\nu G_d(\mathbf{x};\mathbf{x}_0)\sum_{j=0}^{\infty}\nu^j\gamma_j \\ &\sim -2\pi\nu W_{0H}(\mathbf{x}_0) G_d(\mathbf{x};\mathbf{x}_0)\sum_{j=0}^{\infty}[-2\pi\nu R_{d00}]^j \\ &\sim -\frac{2\pi\nu W_{0H}(\mathbf{x}_0)}{1+2\pi\nu R_{d00}} G_d(\mathbf{x}_0;\mathbf{x}_0)\,. \end{aligned} \tag{29a}$$

Equation (29a) agrees with equation (16a) of Principal Result 1. Similarly, upon substituting (28) into the infinite-order inner expansion (20), we obtain

$$v(\mathbf{y};\varepsilon) = \nu W_{0H}(\mathbf{x}_0) v_c(\mathbf{y}) \sum_{j=0}^{\infty}[-2\pi R_{d00}\nu]^j = \frac{\nu W_{0H}(\mathbf{x}_0)}{1+2\pi\nu R_{d00}} v_c(\mathbf{y})\,, \tag{30}$$

which recovers equation (16b) of Principal Result 1.

Next, we compare the results of the hybrid method with results obtained either analytically or numerically from the full perturbed problem (1).

We consider flow in a circular pipe Ω of cross-sectional radius r_0 that contains a concentric core Ω_ε of various cross-sectional shapes centered at the origin. We use Table 1 for the logarithmic capacitance d for a square

core, an elliptical core, and an equilateral triangular core. Using the notation in the table, we set the major and minor semi-axes of the ellipse as $a = 2$ and $b = 1$, and both the side of the square and the equilateral triangle as $h = 1$. To compute the hybrid method solution, we readily calculate that the Green's function is $G_d = -(2\pi)^{-1} \log(r/r_0)$ and that the unperturbed solution is $W_{0H} = \beta(r_0^2 - r^2)/4$. The outer hybrid method solution, as obtained from (16a) of Principal Result 1, is simply

$$w(\mathbf{x};\varepsilon) = \frac{\beta}{4}\left[r_0^2 - r^2 - r_0^2 \frac{\log(r_0/r)}{\log(r_0/[\varepsilon d])}\right], \qquad r = |\mathbf{x}|\,. \tag{31}$$

From (31), we can compute the asymptotic mean flow rate using (2).

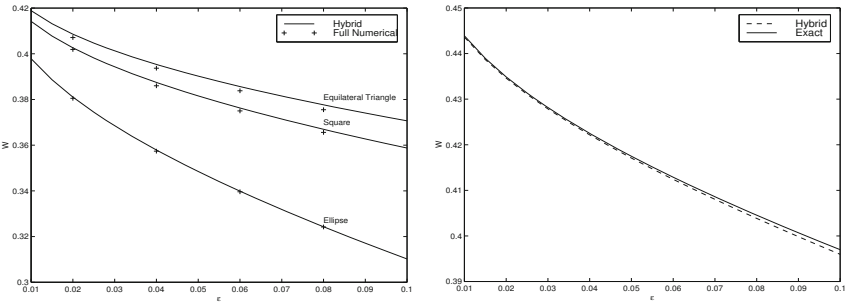

(a) Concentric Geometry: $\bar{w}$ vs. ε (b) Eccentric Geometry: $\bar{w}$ vs. ε

Figure 1. The mean flow velocity $\bar{w}$ versus the cross-sectional 'radius' of an inner core pipe located inside a circular pipe of cross-sectional radius $r_0 = 2$. Left figure: (Concentric annulus geometry). Plots of $\bar{w}$ vs. ε for three different cross-sectional shapes of the inner core pipe. The discrete points are the full numerical results. Right figure (Eccentric Geometry). Plots of $\bar{w}$ versus the circular pipe core cross-sectional radius ε when the inner pipe is centered at $\mathbf{x}_0 = (-1, 0)$. The hybrid and exact results are the dotted and solid curves, respectively.

To validate the asymptotic results for $\bar{w}$, we compare them with corresponding direct numerical results computed from the full problem (1) using the *PDE Toolbox* of MATLAB (1996). For a circular pipe of radius $r_0 = 2$ containing a concentric core and with $\beta = 1$, Fig. 1(a) contains curves of mean flow velocity, $\bar{w}$, versus ε, a measure of the size of the core, for three

different cross-sectional shapes of the core. In the hybrid method solution, the change in shape and size of the core requires only that we vary the product εd, which allows us to compute the entire ε curve very easily. In contrast, for each change of shape and size of the core in the direct numerical solution, we had to re-create the solution geometry and re-mesh the solution grid when using the *PDE Toolbox* of MATLAB (1996). For a core of elliptic cross-section, the figure shows that the hybrid method results agree very well with those of the direct numerical solution. The slight discrepancy in comparing the results for the other two core cross-sectional shapes, the square and equilateral triangle, could be due to the inability of the numerical method to resolve the non-smooth boundary of the core.

Next, we consider flow in a circular pipe Ω of radius $r_0 > 1$ that contains a circular core Ω_ε of radius ε centered at $\mathbf{x}_0 = (-1, 0)$. For this case, the exact mean flow velocity $\bar{w}_E$ for this eccentric annulus geometry can be written as a complicated infinite series as in Ward-Smith (1980). In contrast, we need only calculate three specific quantities for our hybrid formulation in (16). Firstly, the unperturbed solution is again given by $W_{0H}(r) = \beta(r_0^2 - r^2)/4$. Next, since the inner core cross-section is a circle of radius ε, then the logarithmic capacitance is $d = 1$, so that $\nu = -1/\log\varepsilon$. Finally, using the method of images, we solve (13) analytically to obtain the Green's function

$$G_d(\mathbf{x};\mathbf{x}_0) = -\frac{1}{2\pi}\log\left(\frac{|\mathbf{x}-\mathbf{x}_0|r_0}{|\mathbf{x}-\mathbf{x}_0'||\mathbf{x}_0|}\right). \tag{32}$$

Here the image point $\mathbf{x}_0'$ of $\mathbf{x}_0$ in the circle of radius r_0 lies along the ray containing $\mathbf{x}_0$ and satisfies $|\mathbf{x}_0'||\mathbf{x}_0| = r_0^2$. Comparing (32) with (13b), we can then calculate the self-interaction term as

$$R_{d00} \equiv R_d(\mathbf{x}_0;\mathbf{x}_0) = -\frac{1}{2\pi}\log\left[\frac{r_0}{|\mathbf{x}_0-\mathbf{x}_0'||\mathbf{x}_0|}\right]. \tag{33}$$

Substituting (32), (33), $\nu = -1/\log\varepsilon$, and $W_{0H}(r)$, into (16a) we obtain the outer solution for the hybrid method. This solution is then used in (2) with $A_\Omega \sim \pi r_0^2$ to compute the mean flow velocity for the hybrid method. The integral in (2) is obtained from a numerical quadrature. For an eccentric annulus with pipe radius $r_0 = 2$, and with $\beta = 1$, in Fig. 1(b) we plot the mean flow velocity $\bar{w}$ versus the circular core radius ε as obtained from the exact solution and from the hybrid solution. This plot shows that the hybrid method results compare rather well with the exact results.

We remark that for an inner pipe core of an arbitrary shape centered at $\mathbf{x}_0 = (-1, 0)$, the hybrid method solution as obtained above for the eccentric annulus still applies, provided that we replace $\nu = -1/\log\varepsilon$ in (16a) with

$\nu = -1/\log(\varepsilon d)$, where d is to be computed from (7). In particular, if there is an ellipse with semi-axes ε and 2ε centered at $\mathbf{x}_0 = (-1, 0)$ instead of the circle of radius ε, then from Table 1 we get $d = 3/2$. Hence, the plot in Fig. 1(b) for the hybrid solution still applies provided that we replace the horizontal axis in this figure by $3\varepsilon/2$.

3 Some Related Steady-State Problems in Bounded Singularly Perturbed Domains

In this section we extend the analysis of §2 to treat some related steady-state problems. The problem in 3.1, which concerns the distribution of oxygen partial pressure in muscle tissue, involves multiple inclusions in a two-dimensional domain. In §3.2 we show how to extend the method of §2 to a nonlinear problem.

3.1 Oxygen Transport From Capillaries to Skeletal Muscle

The analytical study of tissue oxygenation from capillaries dates from the original work of Krogh (1919). In the oxygen distribution process of the micro-circulation, oxygen binds to its carrier, haemoglobin, in red blood cells, which transports it through the arterioles, branching to the capillary networks, to the collecting venules. In the capillaries, the oxygen is released from its carrier and diffuses into the surrounding tissue. The reviews of Popel (1989), Fletcher (1978), and the references in Titcombe and Ward (2000), provide substantial information on theoretical research in this area.

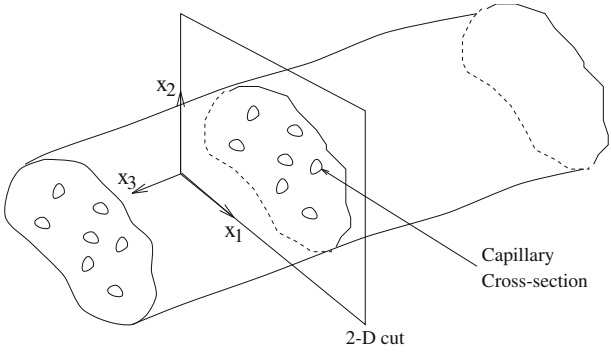

Figure 2. Mathematical idealization of capillary blood supply in skeletal muscle tissue

In this section, we show how to determine the steady-state oxygen partial pressure distribution in a two-dimensional domain representing a transverse section of skeletal muscle tissue that receives oxygen from an array of capillaries of small but arbitrary cross-sectional shape (see Fig. 2). Following the approach of many authors (e.g. Popel (1989)), we model the transport of oxygen from capillaries to tissue by a passive diffusive process. Assuming Fick's law, $J = -D\nabla c$, relating the oxygen flux J to the gradient of oxygen concentration c, and Henry's law, $c = \alpha p$ the dimensionless steady-state oxygen partial pressure p satisfies

$$\triangle p = \mathcal{M}\,, \quad \mathbf{x} \in \Omega \backslash \Omega_p \qquad \Omega_p \equiv \bigcup_{j=1}^{N} \Omega_{\varepsilon_j}\,, \tag{34a}$$

$$\partial_n p = 0, \quad \mathbf{x} \in \partial\Omega\,. \tag{34b}$$

$$\varepsilon \partial_n p + \kappa_j (p - p_{cj}) = 0\,, \quad \mathbf{x} \in \partial\Omega_{\varepsilon_j}\,, \quad j = 1, \ldots, N\,. \tag{34c}$$

The condition (34c) models the capillary wall as a finitely permeable membrane, where $\kappa_i > 0$ is the permeability coefficient of the i^{th} capillary and p_{ci} is the oxygen partial pressure within the i^{th} capillary (assumed constant). In (34c) and (34b), ∂_n is the outward normal derivative to the tissue domain. In deriving (34) we have assumed that the oxygen diffusivity is spatially constant, and so the oxygen consumption rate $\mathcal{M}$ has been normalized by this constant value. To incorporate skeletal muscle tissue heterogeneities, such as localized oxygen-consuming mitochondria, we assume that $\mathcal{M}$ is spatially-dependent and has the form

$$\mathcal{M}(\mathbf{x}) = \mathcal{M}_0 + \sum_{i=1}^{m} \mathcal{M}_i \exp\left(-\frac{|\mathbf{x} - \mathbf{x}_i|^2}{\sigma_i^2} \right)\,, \tag{35}$$

for some positive constants $\mathcal{M}_0$ and $\mathcal{M}_i$ for $i = 1, \ldots, m$.

The model (34) is an extension of the well-known Krogh cylinder model Krogh (1919), which consists of one capillary of circular cross-section concentric with a circular cross-section of muscle tissue. For this concentric annulus geometry $\varepsilon < |\mathbf{x}| < 1$, the exact radially symmetric solution p_e is

$$p_e(r) = p_{c1} + \frac{\mathcal{M}}{2}\left[\frac{r^2 - \varepsilon^2}{2} + \frac{\varepsilon^2 - 1}{\kappa_1} + \log\left(\frac{\varepsilon}{r}\right) \right]. \tag{36}$$

This shows that $p_e = \mathcal{O}(\log \varepsilon)$ as $\varepsilon \to 0$, as induced by the Neumann boundary condition in (34b) on the boundary of the cross-section. In the extended model (34), formulated originally in Titcombe and Ward (2000), one allows for multiple capillaries of arbitrary location, of arbitrary cross-sectional shape, and for the tissue domain to be arbitrary.

Most previous attempts to study the oxygenation of muscle tissue analytically have assumed that the capillaries can be represented as point sources for (34). However, by using the method of matched asymptotic expansions, we show that this type of rough simplification represents only the leading-order term in an infinite asymptotic expansion of the oxygen partial pressure in powers of $-1/\log\varepsilon$, where ε is a measure of the capillary cross-section. From a physiological viewpoint, this type of point-source approximation ignores the effect of the shape of the capillary cross-section and the effect of the interaction between the capillaries. When many capillaries are present, the effect of the capillary interaction should be significant.

Our goal here is to extend the hybrid method of §2 to calculate the asymptotic solution to (34) with an error that is smaller than any power of $-1/\log\varepsilon$. Such an approach, which effectively sums the infinite logarithmic series, takes into account the effect of the capillary interaction.

In the outer region we expand the solution to (34) as

$$p(\mathbf{x};\varepsilon) = P_0(\mathbf{x};\nu_1,\dots,\nu_N) + \sigma(\varepsilon)P_1(\mathbf{x};\nu_1,\dots,\nu_N) + \cdots . \tag{37}$$

Here $\nu_j = \mathcal{O}(1/\log\varepsilon)$ for $j = 1,\dots,N$ are gauge functions to be chosen, and we assume that $\sigma \ll \nu_j^k$ for any $k > 0$ as $\varepsilon \to 0$. Thus, P_0 contains all of the logarithmic terms in the expansion. Substituting (37) into (34a) and (34b), and letting $\Omega_{\varepsilon_j} \to \mathbf{x}_j$ as $\varepsilon \to 0$, we get that P_0 satisfies

$$\triangle P_0 = \mathcal{M}\,, \quad \mathbf{x} \in \Omega\backslash\{\mathbf{x}_1,\dots,\mathbf{x}_N\}\,, \tag{38a}$$

$$\partial_n P_0 = 0\,, \quad \mathbf{x} \in \partial\Omega\,, \tag{38b}$$

$$P_0 \quad \text{is singular as } \mathbf{x} \to \mathbf{x}_j\,. \tag{38c}$$

The matching of the outer and inner expansions will determine singularity behaviors for P_0 as $\mathbf{x} \to \mathbf{x}_j$ for $j = 1,\dots,N$.

In the inner region near the j^{th} capillary Ω_{ε_j} we introduce the inner variables

$$\mathbf{y} = \varepsilon^{-1}(\mathbf{x} - \mathbf{x}_j)\,, \qquad p(\mathbf{y};\varepsilon) = q_j(\mathbf{x}_j + \varepsilon\mathbf{y};\varepsilon)\,, \tag{39}$$

together with the local expansion

$$q_j = p_{cj} + q_{0j}(\mathbf{y};\nu_1,\dots,\nu_N) + \mu q_{1j}(\mathbf{y};\nu_1,\dots,\nu_N) + \cdots . \tag{40}$$

Here we assume that $\mu \ll \nu_j^k$ for any $k > 0$. We then write q_{0j} in the form

$$q_{0j} = A_j q_{cj}(\mathbf{y})\,, \tag{41}$$

where $A_j = A_j(\nu_1,\dots,\nu_N)$ is an unknown constant to be determined, and $q_{cj}(\mathbf{y}) \sim \log|\mathbf{y}|$ as $\mathbf{y} \to \infty$. By substituting (39), (40), and (41), into (34a)

and (34c), we readily derive that q_{cj} is the solution to

$$\triangle_{\mathbf{y}} q_{cj} = 0\,, \quad \mathbf{y} \notin \Omega_j\,; \qquad \partial_n q_{cj} + \kappa_j q_c = 0\,, \quad \mathbf{y} \in \partial\Omega_j\,, \tag{42a}$$

$$q_{cj} \sim \log|\mathbf{y}|\,, \quad \text{as} \quad |\mathbf{y}| \to \infty\,, \tag{42b}$$

where $\Omega_j \equiv \varepsilon^{-1}\Omega_{\varepsilon_j}$. The unique solution to (42) has the following far-field asymptotic behavior:

$$q_{cj}(\mathbf{y}) \sim \log|\mathbf{y}| - \log d_j + \mathcal{O}\left(\frac{1}{|\mathbf{y}|}\right)\,, \quad |\mathbf{y}| \gg 1\,. \tag{42c}$$

In comparing (42) with (7) for the pipe problem of §2, we observe that here $d_j = d_j(\kappa_j)$. For a particular cross-sectional shape of the capillary and for a given value of κ_j, one must compute $d_j = d_j(\kappa_j)$ numerically from a boundary integral method applied to (42). For a circular capillary of radius ε, for which q_{cj} can be found analytically, we readily calculate that

$$d_j = \exp\left(-1/\kappa_j\right)\,. \tag{43}$$

Moreover, by comparing (6b) with (41) we observe that here we have introduced a slight change in the definition of the inner solution. In the analysis below, we will show that $A_j = \mathcal{O}(1)$ as $\varepsilon \to 0$ in (41), which is a direct consequence of the Neumann boundary condition in (34b).

By using (40) and (42c), we re-write the far-field form for $|\mathbf{y}| \gg 1$ of the inner solution in terms of the outer variables as

$$q_j \sim p_{cj} + A_j \log|\mathbf{x} - \mathbf{x}_j| + \frac{A_j}{\nu_j}\,. \tag{44a}$$

Here we have introduced the logarithmic gauge function ν_j by

$$\nu_j \equiv -\frac{1}{\log(\varepsilon d_j)}\,. \tag{44b}$$

The matching condition is that the far-field form (44a) of the inner solution must agree with the near-field behavior of the outer solution for p. Thus, P_0 satisfies (38) subject to the following singularity behavior

$$P_0 \sim p_{cj} + A_j \log|\mathbf{x} - \mathbf{x}_j| + \frac{A_j}{\nu_j}\,, \quad \text{as} \quad \mathbf{x} \to \mathbf{x}_j\,, \quad j = 1, \ldots, N\,. \tag{45}$$

As remarked in §2, we emphasize that the singularity behavior in (45) specifies both the regular and singular part of a Coulomb singularity at each $\mathbf{x}_j$. As such, the singularity behaviors (45) for $j = 1, \ldots, N$ will